Complexity Analysis of Multicarrier and Single-Carrier Systems for Very High-Speed Digital Subscriber Line

Byonghyo Shim and Naresh R. Shanbhag, *Member, IEEE*

***Abstract*—A complexity analysis of discrete multitone (DMT) and single-carrier modulation (SCM) in the context of a very high-speed digital subscriber line (VDSL) is presented in this paper. In addition to the traditional arithmetic complexity measures such as the number of multiply-and-accumulate (MAC) operations, we also compute the memory requirements. Furthermore, we normalize these metrics with respect to the number of information bits transmitted (*rate normalized*) and scale with respect to data path precision (*precision scaled*) in order to obtain more comprehensive metrics. The analysis shows that the number of MAC's per transmitted information bit (N_{MACb}) for SCM is greater than that for DMT for all distances of interest in VDSL. The number of MACs per information bit and scaled with respect to precision (B_{MAC}), i.e., $NB_{\mathrm{MACb}} = N_{\mathrm{MACb}}B_{\mathrm{MAC}}$, was found to be clearly smaller for SCM in loops shorter than approximately 2 kft. This metric was found to be clearly smaller for DMT in loops longer than approximately 3.25 kft. At all lengths, DMT was found to have smaller memory requirements per information bit, as well as smaller precision-scaled memory requirements.**

***Index Terms*—Complexity, discrete multitone, multiply-and-accumulate (MAC), single-carrier modulation, VDSL.**

I. Introduction

VERY high-speed digital subscriber line (VDSL) is the latest digital subscriber line technology that enables high-rate data services over the last mile of the network over unshielded twisted-pair lines [1]–[6]. Supporting both asymmetric and symmetric services with data rates up to 22 Mb/s in the downstream, VDSL holds tremendous potential for serving both residential as well as business customers. In order to achieve tens of megabits per second over conventional copper wire, various state-of-the-art digital modulation technologies are employed.

At the present time, standards for VDSL are developed, and there are two candidate modulation techniques: multicarrier modulation, well-known as discrete multitone (DMT) and single-carrier modulation (SCM), known as quadrature amplitude modulation (QAM) or carrierless AM/PM (CAP) modulation. An extensive study for applying these techniques on VDSL channel has been made [5], [6], and there is an on-going debate regarding achievable data rates [8]–[12] and complexity of two line codes.

In a VDSL system, complexity is an important factor since it impacts the die size and cost. In addition, the optical network unit (ONU) requires low-power consumption (1 *W/line*) to achieve high port densities for economical VDSL deployment. Hence, system complexity becomes important since it is proportional to the power consumption.

The purpose of this paper is to provide a complexity analysis of the two modulation schemes described in VDSL technical specification for DMT [3] and SCM [4]. In analyzing system complexity, we consider the downstream direction from VTU-O transmitter to VTU-R receiver. There have been a few studies on the complexity analysis of two line code [13]–[15]. In [16], the complexity of DMT ADSL and DMT VDSL systems is described in terms of the number of operations (MIPS) in programmable DSP systems. Specifically, our analysis differs from these previous efforts by not only including traditional arithmetic complexity measures such as the number of multiply-and-accumulate (MAC) operations but the memory requirements as well. Furthermore, we normalize these metrics with respect to the number of information bits transmitted and scale it with respect to the precision in order to obtain complexity metrics that are comprehensive.

Employing the symbol period as a unit of time, we denote N_{MAC} and N_{MEM} as the number of multiply-accumulates (MACs) and memory locations required to transmit a symbol. As the number of bits per symbol are usually different for DMT and SCM, we propose N_{MACb} and N_{MEMb} (henceforth referred to as *rate normalized* metrics) as the number of MACs and number of memory locations, respectively, needed per transmitted information bit, i.e.,

$$N_{\mathrm{MACb}} = \frac{N_{\mathrm{MAC}}}{b_{\mathrm{symb}}} \tag{1}$$

$$N_{\mathrm{MEMb}} = \frac{N_{\mathrm{MEM}}}{b_{\mathrm{symb}}} \tag{2}$$

where b_{symb} is the number of bits per symbol. Further, in order to account for precisions, we propose the following two complexity metrics (henceforth referred to as *precision scaled* metrics)

$$NB_{\mathrm{MACb}} = N_{\mathrm{MACb}}B_{\mathrm{MAC}} \tag{3}$$

$$NB_{\mathrm{MEMb}} = N_{\mathrm{MEMb}}B_{\mathrm{MEM}} \tag{4}$$

Manuscript received August 20, 2001; revised September 5, 2002. This work was supported by the National Science Foundation under Grant CCR 99–79381. The associate editor coordinating the review of this paper and approving it for publication was Dr. Naofal M. W. Al-Dhahir.

The authors are with the Coordinated Science Laboratory and the Department of Electrical and Computer Engineering, University of Illinois at Urbana-Champaign, Urbana, IL 61801 USA (e-mail: bshim@mail.icims.csl.uiuc.edu; shanbhag@mail.icims.csl.uiuc.edu).

Digital Object Identifier 10.1109/TSP.2002.806583

TABLE I
PARAMETERS OF A DMTVDSL SYSTEM

parameter	specification
FFT size (N)	8192
Number of tones ($\frac{N}{2}$)	4096
Tone width (Δf)	4.3125 kHz
Cyclic extension length (ν)	640
Sampling rate (f_s)	35.328 MHz
Bandwidth	17.664 MHz
Duplexing	FDD
# of bits/tone	$1 \sim b_{max}$ $(8 \le b_{max} \le 15)$

where B_{MAC} and B_{MEM} are the precisions of the MAC and the number of bits per word in the memory, respectively.

The organization of this paper is as follows: in Section II, we briefly review the signal processing blocks of a multi-carrier system and analyze its complexity. In Section III, the single-carrier system is analyzed in a similar manner. In Section IV, we provide the comprehensive complexities of the two line codes and we conclude in Section V.

II. COMPLEXITY ANALYSIS OF DMT

A. Overview

DMT employs a large number of carriers with each being individually quadrature amplitude modulated. The parameters of a DMT based VDSL system [3] are shown in Table I.

The block diagram of a typical DMT system is shown in Fig. 1. In the transmitter, the input data bits b_k is mapped onto QAM constellation points with up to 11 bits per tone in order to generate the frequency domain samples $X_k (k = 0, \ldots, N-1)$. Each tone has a complex transmit gain to control the tone power. As the number of tones equal $N/2$, N real multiplications are required for transmit gain scaling and $N/2$ memory locations are required each for the bit-allocation table and gain constants.

The frequency domain samples X_k are converted into a time domain symbol by applying an N-point inverse FFT (IFFT)

$$x_n = \sum_{k=0}^{N-1} X_k W_N^{-kn}, \quad n = 0, 1, \ldots, N-1, \tag{5}$$

where x_n is the time domain sample, X_k is the frequency domain sample and $W_N^{-kn} = e^{j2\pi kn/N}$. For a real sequence x_n, X_k has the conjugate symmetry property

$$X_i = X_{N-i}^*, \quad 0 < i < \frac{N}{2}, \tag{6}$$

which enables an N-point IFFT to be implemented via an $N/2$-point complex IFFT with an additional butterfly operation for the preprocessing stage [17]. Since $N/4$ multiplications are required in each butterfly stage and there are $\log_2(N/2)+1$ butterfly stages including the preprocessing butterfly stage, a total of $(N/4)\log_2 N$ complex multiplications (or $0.75N\log_2 N$ real multiplications) are needed.[1] Similar complexity is required for the N-point FFT operation at the receiver. For the FFT/IFFT operation, assuming in-place computation and exploiting the odd symmetry in the transform coefficients, one can show that $3N/4$ complex memory locations are required for coefficient storage.

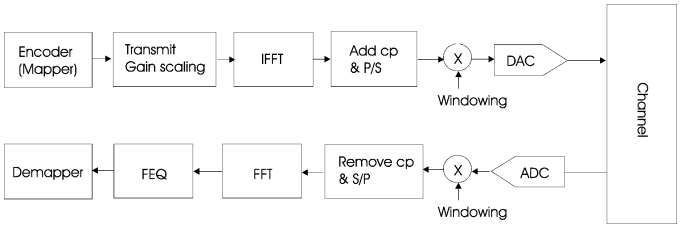

Fig. 1. DMT VDSL transceiver.

A cyclic extension is added to the time domain symbol to reduce intersymbol interference. Next, windowing is applied to reduce out-of-band leakage [18]. This operation requires 2ν multiplications and memory locations. The resulting signal is then passed through a digital-to-analog converter and transmitted.

In the receiver, after the analog-to-digital converter (ADC), the received signal is shaped via a window function in order to reduce interchannel interference. Note that a time-domain equalizer is generally unnecessary in VDSL DMT as the channel impulse response is shorter than the recommended cyclic prefix length. Received symbols are transformed into frequency domain via an FFT operation. Due to channel impairments, signals in each subchannel undergo attenuation and phase rotation during transmission. The frequency domain equalizer (FEQ) inverts the channel with a complex multiplication for each tone, which can be achieved by 3 real multiplications per tone [19]. In the FEQ, N complex memory locations are required for data and coefficients. The decision device then detects the symbols in each tone. The overall complexity of the DMT system is summarized in Table II.

B. ADC Precision

Assuming a uniform quantization noise model, the signal-to-quantization noise ratio (SQNR) at the ADC output is given by [22]

$$\mathrm{SQNR} = 6.02B_{\mathrm{ADC}} + 4.77 - \mathrm{PAR[dB]} \tag{7}$$

where B_{ADC} is the ADC precision, PAR is the peak-to-average ratio defined as $10\log A_{\mathrm{peak}}^2/E[r(t)^2]$, where the dynamic range of the ADC output is $[-A_{\mathrm{peak}}, A_{\mathrm{peak}}]$ and $r(t)$ is the received signal. Since the absolute peak does not occur very frequently in practice, a realistic value for the PAR can be determined by specifying the probability of clipping P_{clip}.

Since the probability density function of the DMT signal is well approximated as a Gaussian, P_{clip} can be expressed as

$$P_{\mathrm{clip}} = 2Q\left(\frac{A_{\mathrm{peak}}}{\sqrt{E[r(t)^2]}}\right) \tag{8}$$

[1]Employing strength reduction, direct multiplication of two complex numbers $(a+bj)\cdot(c+dj) = (ac-bd)+j(ad+bc)$ is transformed into $(a-b)d+a(c-d) = ac-bd$, $(a-b)d+a(c+d) = ad+bc$ and hence one multiplication can be saved at the expense of three additions [19].

TABLE II
COMPLEXITY OF A DMT SYSTEM

MAC operation block	N_{MAC}	N_{MEM}
Transmit gain scaling	N	N
IFFT	$0.75Nlog_2N$	$1.5N$
Tx-windowing	2ν	2ν
Rx-windowing	2ν	2ν
FFT	$0.75Nlog_2N$	N
FEQ	$1.5N$	$2N$
Total	$2.5N + 1.5Nlog_2N + 4\nu$	$5.5N + 4\nu$

where $Q(y) = 1/\sqrt{2\pi}\int_y^\infty e^{-1/2x^2}dx$, and hence PAR is given by

$$\text{PAR} = \left[Q^{-1}\left(\frac{P_{\text{clip}}}{2}\right)\right]^2. \tag{9}$$

For a typical clipping probability of 10^{-7}, PAR computes to 14.5 dB from (9)[2].

Since $\text{SNR}_i = \sigma^2_{r_i}/(\sigma^2_{\text{qnt,ADC}} + \sigma^2_{\text{noise}})$, the relationship between the SNR and SQNR at the receiver input is given by

$$\text{SQNR} = \text{SNR}_i + 10\log\left(1 + \frac{1}{r}\right)\text{[dB]} \tag{10}$$

where the quantization noise power to channel noise power ratio r is defined as $r = \sigma^2_{\text{qnt,ADC}}/\sigma^2_{\text{noise}}$. In VDSL, the dominant source of noise power σ^2_{noise} is due to far-end crosstalk (FEXT). The power of FEXT σ^2_{FEXT} is expressed as [1]

$$\sigma^2_{\text{FEXT}} = \int_{B_{\min}}^{B_{\max}} \text{PSD}^2_{tx}|H(f)|^2\left(\frac{N_d}{49}\right)^{0.6} Kdf^2df \tag{11}$$

where N_d is the number of disturbers, K is coupling constant, d is the line length, and channel loss in decibel is typically $10\log|H(f)|^2 = d(-6.0\sqrt{f} + 0.07f)$.

The SQNR needs to be higher than the subchannel SNR_i in order to minimize the impact of ADC quantization noise on the BER. If the degradation in SNR due to quantization noise is to be limited to 0.25 dB [18], i.e.,

$$\text{SQNR} > \max_i \text{SNR}_i + 12.27\text{[dB]}. \tag{12}$$

From (7) and (12), the ADC precision is obtained as

$$B_{\text{ADC}} = \left\lceil \frac{1}{6.02}(\max_i \text{SNR}_i + \text{PAR} + 7.5) \right\rceil. \tag{13}$$

The ADC precision in DMT is determined by the subchannel with the highest SNR because each subchannels needs to have the same BER.

[2]Various methods to reduce PAR are suggested [20], [21]. We do not consider these techniques since employing them increases the complexity of the signal processing blocks.

The number of bits in a subchannel i is given by [12]

$$b_i = \log_2\left(1 + \frac{\text{SNR}_i \cdot \gamma_c}{\Gamma \cdot \gamma_m}\right) \tag{14}$$

where Γ is the SNR gap, γ_m is the system margin, and γ_c is the coding gain. For a bit error rate of 10^{-7}, the required SNR in subchannel i approximates to

$$\text{SNR}_i = 10\log(2^{b_i} - 1) + 9.8 + \gamma_m - \gamma_c. \tag{15}$$

Employing (7), (12), and (15), we have the following approximate expression for the ADC precision

$$B_{\text{ADC}} \sim \left\lceil \frac{1}{6.02}(3b_{\max} - \gamma_c + \gamma_m + \text{PAR} + 17.3) \right\rceil. \tag{16}$$

The draft standards [1], [3] specify a noise margin of 6 dB and the coding gain of approximately 3 dB. As the maximum number of bits per subchannel is constrained as: $8 \le b_{\max} \le 15$, from (16), the ADC in a DMT system requires $10 \sim 14$ bit precision.

C. Internal Precision

Since digital processing in a DMT system is performed primarily in the FFT/IFFT blocks, the quantization noise of the FFT should be less than the ADC quantization noise, i.e.,

$$\text{SQNR}_{\text{FFT}} > \text{SQNR}. \tag{17}$$

When implementing an FFT in fixed-point arithmetic, scaling is needed to guard against overflow in the butterfly computations. If an appropriate scaling scheme is employed, SQNR_{FFT} can be expressed as [22]

$$\begin{aligned}\text{SQNR}_{\text{FFT}} &= 10\log\left(\frac{2^{2B_{\text{FFT}}}}{16N}\right)\\ &= 6.02B_{\text{FFT}} - 12.04 - 10\log N.\end{aligned} \tag{18}$$

Substituting (7) and (18) into (17), we get

$$B_{\text{FFT}} > \lceil B_{\text{ADC}} + 1.67\log N - 0.17\text{PAR} + 2.8\rceil. \tag{19}$$

As supported in Fig. 2, (19) indicates that doubling the FFT size N necessitates 0.5 additional bits in order to maintain SQNR. With PAR$= 14.5$ dB, $B_{\text{ADC}} = 10 \sim 14$ bits, and $N = 8192$, we obtain the required precision $B_{\text{FFT}} = 17 \sim 21$ bits.

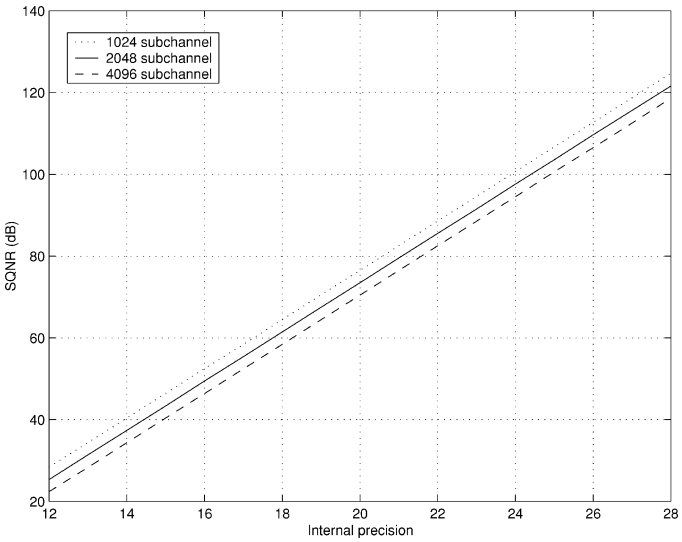

Fig. 2. SQNR of a fixed-point FFT obtained via simulations.

D. Complexity Analysis

The relationship between the sampling frequency and the bit-rate in DMT (referred to as the *rate constraint*) is given by

$$\frac{b_{\text{symb}}}{R} = T_{\text{symb}} = \frac{N+\nu}{f_s} \tag{20}$$

where ν is the number of samples in the cyclic extension, $b_{\text{symb}} = \sum_i b_i$ is the total number of bits per symbol, and $f_s = \Delta f N$ is the sampling frequency.

The duration of the cyclic extension is chosen to be greater than the channel delay spread T_d in order to prevent ISI, i.e.,

$$\frac{\nu}{f_s} \geq T_d. \tag{21}$$

In addition, the block size N should be chosen such that the cyclic extension results in minimal loss in throughput, i.e.,

$$\nu = \frac{\alpha}{1-\alpha} N \tag{22}$$

where α is typically 5–7%. From (21) and (22), we obtain the *throughput loss* constraint

$$N \geq \frac{1-\alpha}{\alpha} T_d f_s. \tag{23}$$

Substituting (22) in (20), we get

$$N = T_{\text{symb}} f_s (1-\alpha). \tag{24}$$

Note that (23) and (24) indicate that $T_{\text{symb}} \geq T_d/\alpha$, i.e., the symbol period should be sufficiently larger than the delay spread. In any case, (24) implies that N increases with the delay spread of the channel T_d. Using (20), (22) and Table II, we have the rate normalized arithmetic complexity N_{MACb} as follows:

$$N_{\text{MACb}} = \left[\frac{(2.5+1.5\log_2 N)(1-\alpha)+4\alpha}{R}\right] f_s \tag{25}$$

TABLE III
PARAMETERS OF A SCM VDSL

parameter	specification
Modulation	Passband spectral shaping or Baseband spectral shaping
Constellation size	$4 \sim 256$
Carrier frequency	scalable (granularity of 33.75KHz)
Symbol rate	scalable (granularity of 67.5Kbaud)
Duplexing	FDD with 2 up/down band

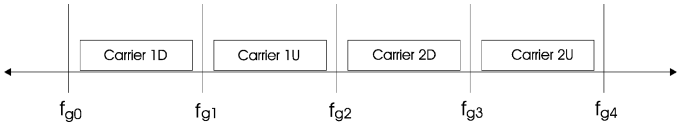

Fig. 3. VDSL spectral plan for 998 where $f_{g0} = 0.138$ MHz, $f_{g1} = 3.75$ MHz, $f_{g2} = 5.2$ MHz, $f_{g3} = 8.5$ MHz, $f_{g4} = 12.0$ MHz.

where N is given by (24). Similarly, the rate normalized memory complexity N_{MEMb} is given by

$$N_{\text{MEMb}} = \left[\frac{5.5(1-\alpha)+4\alpha}{R}\right] f_s. \tag{26}$$

The precision scaled arithmetic and memory complexity metrics are then obtained as

$$NB_{\text{MACb}} = B_{\text{FFT}}^2 \left[\frac{(2.5+1.5\log_2 N)(1-\alpha)+4\alpha}{R}\right] f_s \tag{27}$$

and

$$NB_{\text{MEMb}} = B_{\text{FFT}} \left[\frac{5.5(1-\alpha)+4\alpha}{R}\right] f_s \tag{28}$$

where B_{FFT} is given by (19). Note that the complexity of $m \times m$ multiplier is given by $O(m^2)$[23].

III. Complexity Analysis of SCM

SCM [24]–[27] includes carrierless AM/PM (CAP) based on passband spectral shaping and quadrature amplitude modulation (QAM) based on baseband spectral shaping. The parameters of an SCM based VDSL system [4] are shown in Table III. Since there are no substantial differences between QAM and CAP, without loss of generality, we consider the CAP system (see Fig. 4) in this paper.

A. Overview

Both DMT and SCM for VDSL employ frequency-division duplexing (FDD) which partitions the frequency spectrum into two upstream and downstream transmission bands as shown in Fig. 3 [4]. In each of the bands in SCM, a maximum of 8 bits/symbol can be allocated. These symbols are modulated in

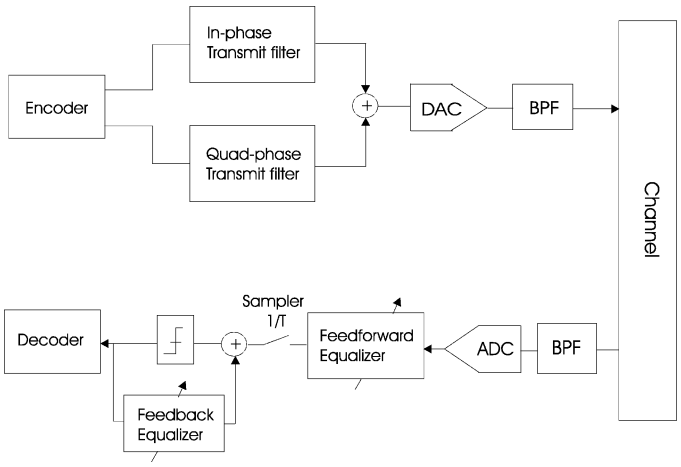

Fig. 4. CAP VDSL transceiver.

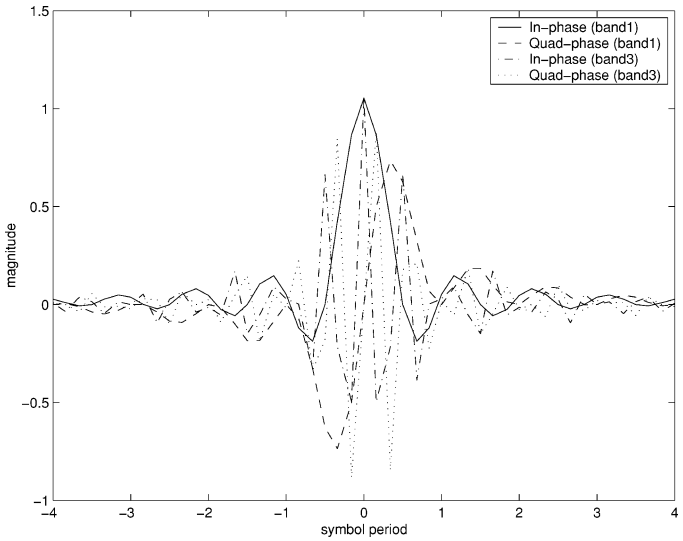

Fig. 5. Impulse response of the transmit filter in SCM.

the digital domain via pulse-shaping filters. The in-phase and quadrature-phase filters are designed to form a Hilbert pair. The transmitted signal is expressed as

$$s(t) = \sum_{k=-\infty}^{\infty} (a_k p(t-kT) - b_k q(t-kT)) \tag{29}$$

where a_k and b_k are discrete multilevel symbols at time kT, $p(t)$ and $q(t)$ are impulse responses of the in-phase and quadrature-phase pulse-shaping filters, respectively. The passband impulse responses $p(t)$ and $q(t)$ are given by (see Fig. 5)

$$\begin{aligned} p(t) &= g(t)\cos(2\pi f_c t) \\ q(t) &= g(t)\sin(2\pi f_c t) \end{aligned} \tag{30}$$

where f_c is the carrier frequency and $g(t)$ is the square-root raised cosine filter with a roll-off factor α and bandwidth $(1+\alpha)/2T$, where T is the symbol period.

If we assume the number of taps in a transmit pulse-shaping filter to be N_{tx}, $2N_{tx}$ multiplications and $4N_{tx}$ memory locations are required in each band. Note that for the disparity between the symbol rate in each transmit band, the transmit filter includes an interpolator to perform digital upsampling operation [28].

At the receiver, the sampled and decimated signal is fed to a decision feedback equalizer (DFE). The DFE is composed of a parallel combination of two adaptive feedforward and feedback FIR filters. While the feedback filters operate at a symbol rate of $f_{\text{symb}} = 1/T_{\text{symb}}$, the feedforward filters usually operate at a multiple of the symbol rate $f_s = m * f_{\text{symb}}$, where m is the oversampling factor. As shown in Fig. 4, the feedforward filter and feedback filter work together to equalize the channel distortion and compensate for time-varying narrowband radio frequency interference (RFI).

If we assume the number of filter taps of the feedforward and feedback filters to be N_{ff} and N_{fb}, respectively, then $2N_{ff}$ and $3N_{fb}$ multiplications [19] are required for equalization in the receiver. In addition, $3N_{ff}$ and $4N_{fb}$ memory locations are required for the feedforward and feedback filters, respectively. We do not consider the complexity of the coefficient update block since this operation is performed infrequently in steady state.

After equalization, the decision device (slicer) converts the equalized signal into data symbols which are subsequently decoded. The complexity of an SCM system is summarized in Table IV.

To achieve reasonable performance, the overall equalizer length needs to be greater than the channel impulse response. If we restrict our attention to the feedforward equalizer only, the feedforward filter should span the delay spread T_d of channel impulse response. Thus, we approximately have

$$N_{ff} \geq T_d f_s \tag{31}$$

where we set T_d as the duration that accounts for 99% of the total channel impulse response power.

In general, the feedforward and feedback filters in a DFE equalize the precursor and postcursor ISI, respectively. Fig. 6 shows the channel impulse response for the 1 kft and 4 kft length of 26-gauge line [1]. The number of taps increases with delay spread thereby increasing the complexity of SCM.

B. ADC Precision

Equation (13), derived for a DMT system, applies to SCM as well but with the following difference. The receiver input SNR is computed for each band and PAR is typically smaller. Fig. 7 compares the probability distribution function of an SCM transmit signal with a 256-point constellation in band1 and a 64-point constellation in band3 with that of a DMT system with 4096 tones. As going from single-band to two-band FDD scheme, PAR of SCM increases considerably. However, as can be seen, the distribution of SCM is narrower than that of DMT. For a clipping probability of 10^{-7}, the PAR ratio of SCM is about 10.3 dB.

The SNR at the receiver front-end is given by

$$\text{SNR} = 10\log\frac{\sigma_{rx}^2}{N_0 + \sigma_n^2} \tag{32}$$

where $\sigma_{rx}^2 = \int_{B_{\min}}^{B_{\max}} \text{PSD}_{tx}|H(f)|^2 df$ is the received signal power, PSD_{tx} is the transmission power spectral density, $|H(f)|^2$ is the power of the channel transfer function, N_0 is

TABLE IV
COMPLEXITY OF AN SCM SYSTEM

MAC operation block	N_{MAC}	N_{mem}
Tx pulse-shaping FIR filter	$2N_{tx}$	$4N_{tx}$
Rx feedforward FIR filter	$2mN_{ff}$	$3mN_{ff}$
Rx feedback FIR filter	$3N_{fb}$	$4N_{fb}$
Total	$2N_{tx} + 2mN_{ff} + 3N_{fb}$	$4N_{tx} + 3mN_{ff} + 4N_{fb}$

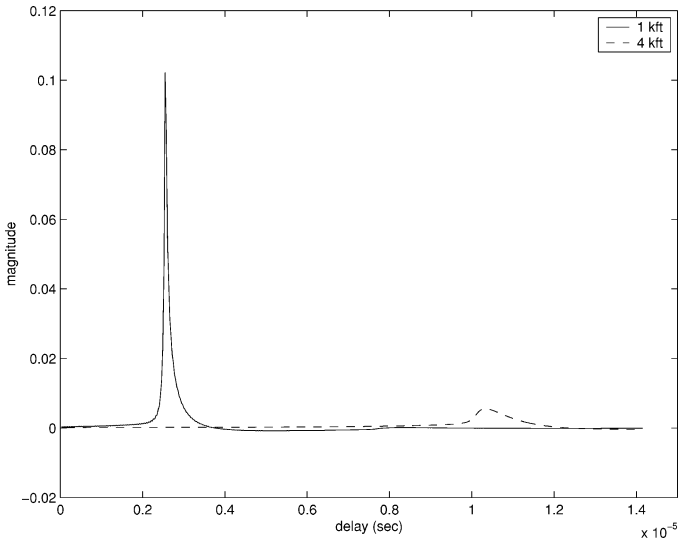

Fig. 6. Channel impulse response of a 26-gauge cable.

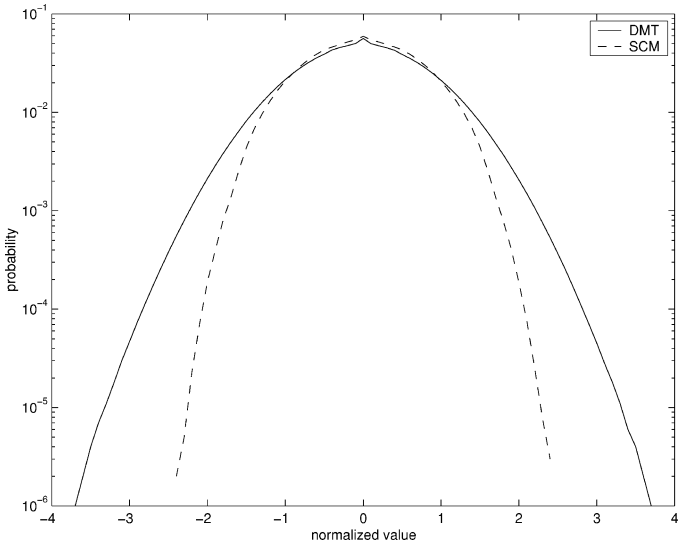

Fig. 7. Probability distribution function of the transmit signal amplitude in DMT and SCM.

the AWGN power, and σ_n^2 is the power of other crosstalks including FEXT in (11).

For the downstream band 1 shown in Fig. 3 and ANSI specified noise model A [1] with 20 VDSL FEXT disturbers, the SNR at short distance ($d = 1$ kft) computes to 36.8 dB. Substituting SNR$=$ 36.8 dB, $PAR = 10.3$ dB into (13) results in $B_{\mathrm{ADC}} = 10$ bits.

Since SCM employs FDD, the signal power at the receiver front-end increases due to the ingress in adjacent frequency bands. Thus, it degrades performance and increases the ADC precision. In order to alleviate this problem, a guard band between the upstream and downstream band and an analog bandpass filter are used [4], [29].

C. Internal Precision

Since the inputs of the feedback filter are the slicer outputs which require only 4 bits for each I and Q channels, it is the feedforward filter that dominates the arithmetic complexity.

Let $\boldsymbol{X} = [x_0\ x_1\ \cdots\ x_{N-1}]$ and $\boldsymbol{W} = [w_0\ w_1\ \cdots\ w_{N-1}]$ be an $N \times 1$ received input and coefficient vector, respectively, and assume that y is the filter output given by $y = \boldsymbol{W}^T\boldsymbol{X}$, then the error signal in feedforward filter is

$$\varepsilon = y_d - \boldsymbol{W}^T\boldsymbol{X} \tag{33}$$

where y_d is the desired output.

In order to reduce the impact of quantization noise on the BER, the mean square quantization error J_{qnt} should be much smaller than the mean square error with infinite precision $J_{inf} = E(\varepsilon^2)$ [30].

$$J_{qnt} \ll J_{inf}. \tag{34}$$

The mean square quantization error J_{qnt} in the filter output y can be expressed as

$$\begin{aligned} J_{qnt} =& E[\Delta y^2] \\ =& E[\Delta\boldsymbol{W}^T\boldsymbol{X}(\Delta\boldsymbol{W}^T\boldsymbol{X})^T] \end{aligned} \tag{35}$$

where $\Delta\boldsymbol{W}$ and Δy are the coefficient quantization error vector and the output quantization error vector, respectively. We assume that the coefficient quantization errors have zero mean with variance $\sigma_{qnt}^2 = 2^{-2B_f}/3$, where B_f is the coefficient precision. In addition, we assume that the received signal and the quantization error in the coefficients are uncorrelated. With these assumptions, we have

$$J_{qnt} = N\sigma_{qnt}^2\sigma_x^2 \tag{36}$$

where σ_x^2 is received input signal power. Inserting (36) into (34), we can show that

$$\begin{aligned} B_f \geq& 1.67\log\left(\frac{N\sigma_x^2}{3J_{inf}\beta}\right) \\ =& 0.17\mathrm{SNR} + 1.67\log N + 1.67\log\left(\frac{\rho}{3\beta}\right) \end{aligned} \tag{37}$$

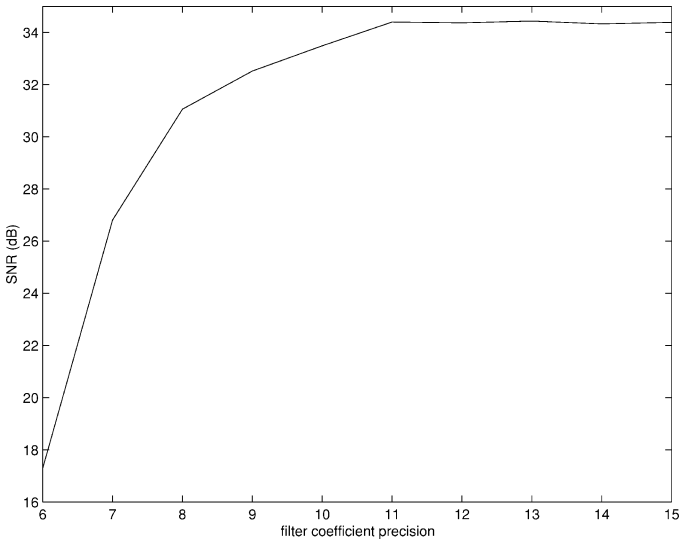

Fig. 8. Output SNR of the feedforward equalizer versus coefficient precision.

where the output SNR is defined as $10\log(\sigma_d^2/J_{inf})$, σ_d^2 is the desired signal power, β is the margin needed to minimize finite-precision effects, and $\rho = \sigma_x^2/\sigma_d^2$ is the receiver input to output signal power ratio.

Since B_f is linearly dependent on SNR, a channel with short distance usually requires maximum precision. In order to minimize the finite-precision effects, we chose $\beta = 0.023$, which results in 0.1 dB between infinite and finite precision performance. An AGC setting is assumed such that ρ becomes unity. For an SNR of 34.3 dB and 64 feedforward taps in 2 kft channel, (37) indicates that a 11 bit coefficient precision is required. This is supported by simulation results in Fig. 8, where the desired performance is achieved with 11 bits of precision.

D. Complexity Analysis

In SCM

$$b_{\text{symb,i}} = \log_2 M_i \tag{38}$$

where $b_{\text{symb,i}}$ is the number of bits per symbol and M_i is the constellation size, respectively, for the ith band.

Using the results of Table IV, we obtain the expression for the rate normalized complexity metric N_{MACb} as

$$N_{\text{MACb}} = \frac{\sum_i (2N_{tx_i} + 2mN_{ff_i} + 3N_{fb_i})}{\sum_i \log_2 M_i}. \tag{39}$$

Similarly, the rate normalized memory complexity N_{MEMb} is given by

$$N_{\text{MEMb}} = \frac{\sum_i (4N_{tx_i} + 3mN_{ff_i} + 4N_{fb_i})}{\sum_i \log_2 M_i}. \tag{40}$$

The precision scaled arithmetic and memory complexity metrics are then obtained as

$$NB_{\text{MACb}} = B_f B_{\text{ADC}} \frac{\sum_i (2N_{tx_i} + 2mN_{ff_i} + 3N_{fb_i})}{\sum_i \log_2 M_i} \tag{41}$$

and

$$NB_{\text{MEMb}} = B_f \frac{\sum_i (4N_{tx_i} + 3mN_{ff_i} + 4N_{fb_i})}{\sum_i \log_2 M_i} \tag{42}$$

where B_f and B_{ADC} are given by (37) and (13), respectively.

IV. Discussion

In the previous sections, we have analyzed the complexity of DMT (see Table II) and SCM (see Table IV) VDSL systems that satisfy the corresponding draft standards in [3] and [4], respectively. In this section, we employ these results in order to evaluate the complexity of DMT and SCM as a function of the channel length (delay spread T_s).

Given a channel delay spread T_d and the relation $T_{\text{symb}} > T_d/\alpha$, (23) indicates that

$$N \geq \frac{T_d f_s (1-\alpha)}{\alpha}$$

whereas (31) indicates that for SCM the equalizer tap length is given by

$$N_{ff} \geq T_d f_s.$$

Assuming that the transmit spectra are the same for both systems, N is much greater than N_{ff}. However, FFT algorithms reduce the computational complexity of DMT to $O(N \log_2 N)$. In addition, $b_{\text{symb}} = \sum_i b_i$ in downstream band 1 and 3 of DMT at 1 kft is approximately given by

$$b_{\text{symb,DMT}} \approx 13\,300$$

whereas for SCM

$$b_{\text{symb,SCM}} \approx 14$$

indicating that the number of bits per symbol in DMT is much larger than SCM. Thus, we can expect the rate normalized complexity of DMT to be in general smaller than that of SCM.

To evaluate the overall complexity of two line code, we simulated these schemes for various VDSL channel conditions. The system parameters used in the simulations are listed in Tables I and III, where we used maximum 11 bit per tone ($b_{\max} = 11$ and, hence, 12 bits ADC) in DMT and maximal allowable symbol rate ($f_{\text{symb}} = N \cdot 67.5\,\text{kHz}$, where $N = \max_n BW > 67.5\,n\,\alpha\text{kHz}$, α is roll-off factor) in SCM for a comparable bandwidth. First, we considered a single 24-gauge VDSL channel with AWGN and self-FEXT from 20 other users. In DMT, we computed the bit loading tables [31] assuming an *SNR* gap of 9.8 dB, a noise margin of 6 dB, and a coding gain of 3 dB. In SCM, we considered only the feedforward equalizer with N_{ff} taps determined according to (31). For both systems, the downstream band1 and 3 of spectral plan 998 shown in Fig. 3 is employed [4].

Fig. 9(a) plots the rate normalized metrics N_{MACb} and N_{MEMb} given in (25)–(26) for DMT and (39)–(40) for SCM. As expected, we find that DMT is better than the SCM overall with the difference increasing with N. When precision scaled complexity metrics are considered [(27)–(28) for DMT and

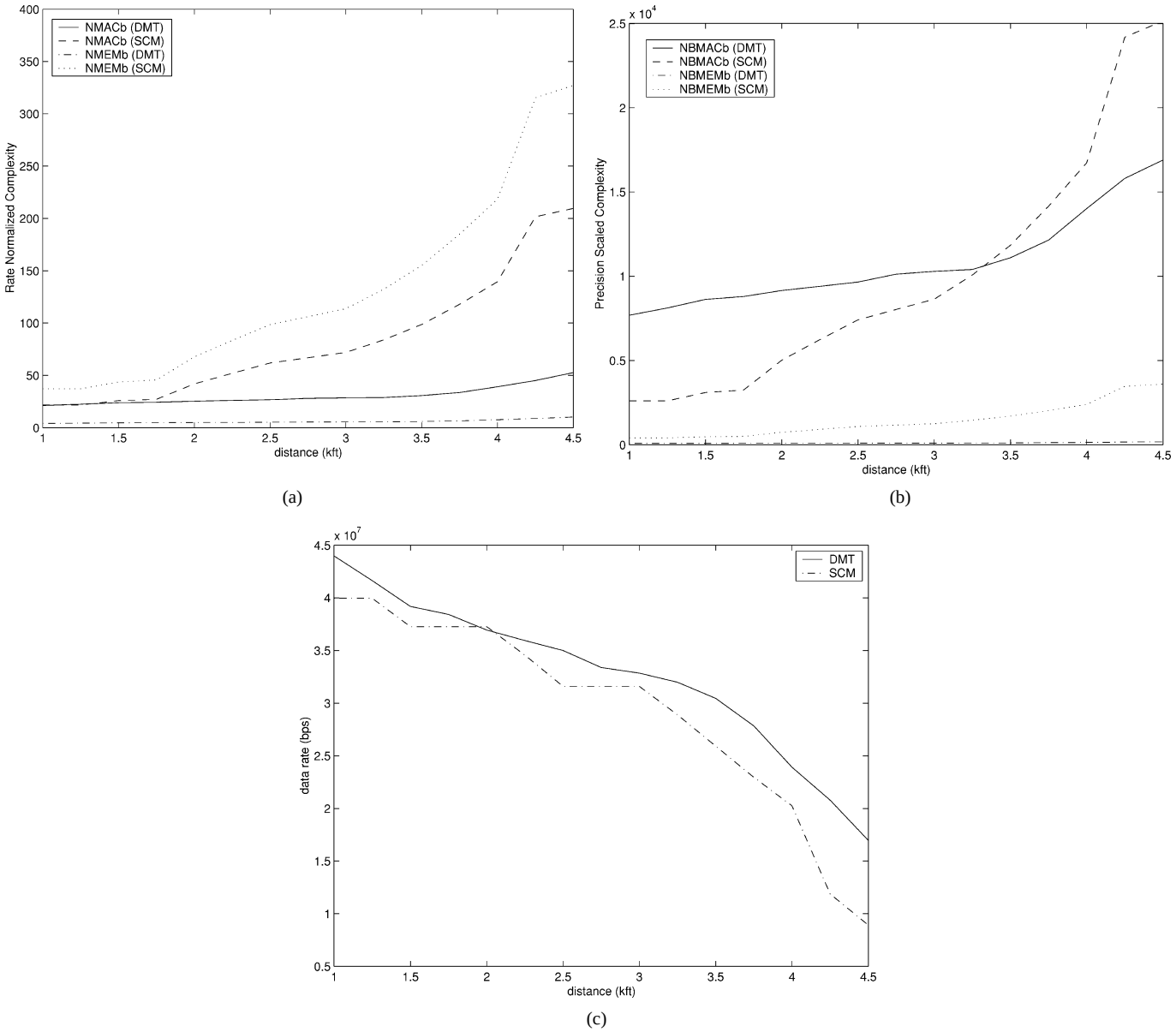

Fig. 9. Complexity metrics for DMT and SCM as a function of cable length. (a) Rate normalized complexity metrics (N_{MACb} and N_{MEMb}). (b) Precision scaled complexity metrics (NB_{MACb} and NB_{MEMb}). (c) Data rate (R_{DMT} and R_{SCM}).

(41)–(42 for SCM], we find from Fig. 9(b) that DMT is also better in memory complexity. However, we observe that SCM has a lower computational complexity than DMT for cable lengths of up to 3.25 kft. For distances longer than 3.25 kft, DMT has a lower computational complexity as well as a lower memory complexity.

We next considered a VDSL channel having mixed gauge and bridge tap. Bridge tap is an open-ended twisted pair, which is connected in shunt with a working loop. Bridge taps are usually located near the customer premises with length varying from tens to hundreds feet [32]. As shown in Fig. 10, the bridge tap introduces deep nulls at odd multiples of a certain frequency and thereby attenuates the transmitted signal more severely. In addition, a fraction of the incident signal is reflected back to the transmitter and, therefore, attenuates the signal. In order to handle these nulls, DFE needs to be employed in SCM and a corresponding subchannel b_i should be reduced or turned off in DMT. As the feedback filter with proper taps performs as well as any longer size due to the finite length of channel response [34], we set the size of feedback filter taps at the point where performance converges. Fig. 11 shows the complexity and performance results for the case where bridge tap with mixed gauge (24 to 26 gauge) is located at 150 ft from the customer premises end. We observe that SCM maintains its advantage in computational complexity for a distance less than 3 kft.

As a worst case scenario, a channel where radio frequency interference (RFI) is present was considered. Since VDSL overlaps an amateur radio band, a copper wire acts as an antenna attracting the narrowband radio signal into the VDSL receiver and radiating the transmit signal into the radio station. As an amateur radio receiver is very sensitive, unwanted radiation of the VDSL signal may severely harm the communications. In order to suppress the RF egress into the amateur radio receiver, transmit PSD in these RFI bands should be attenuated (down to

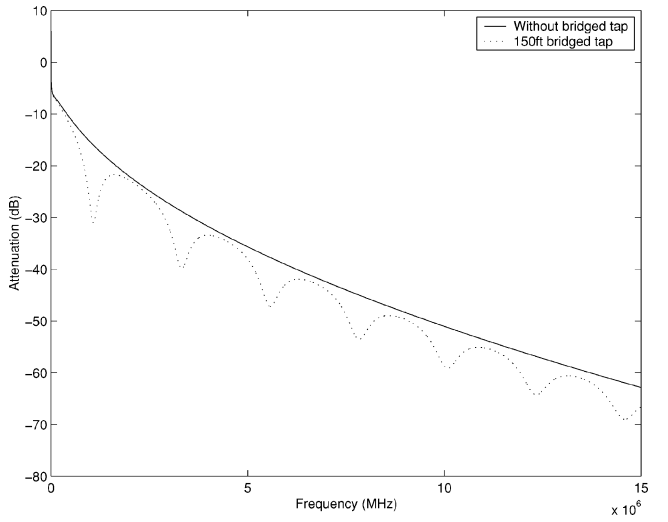

Fig. 10. Attenuation of 26- and 24-gauge mixed loop (2 kft) with and without 150-ft bridge tap.

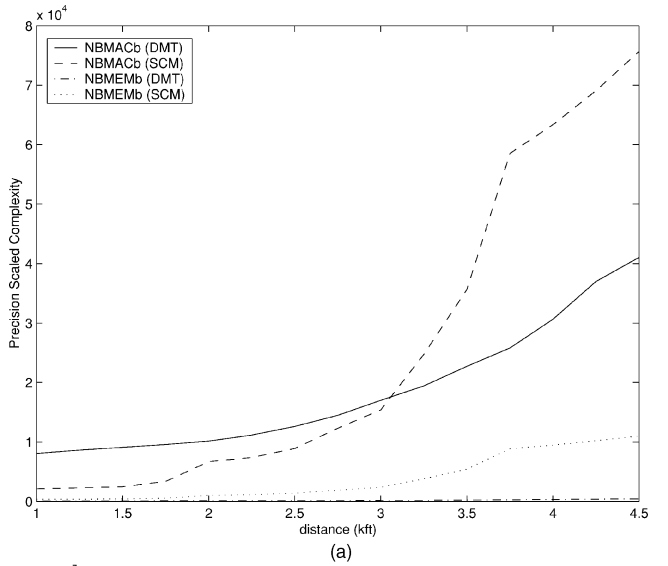

Fig. 11. Complexity metrics and performance when mixed-gauge and 150 ft bridge tap is employed. (a) Precision scaled complexity metrics (NB_{MACb} and NB_{MEMb}). (b) Data rate (R_{DMT} and R_{SCM}).

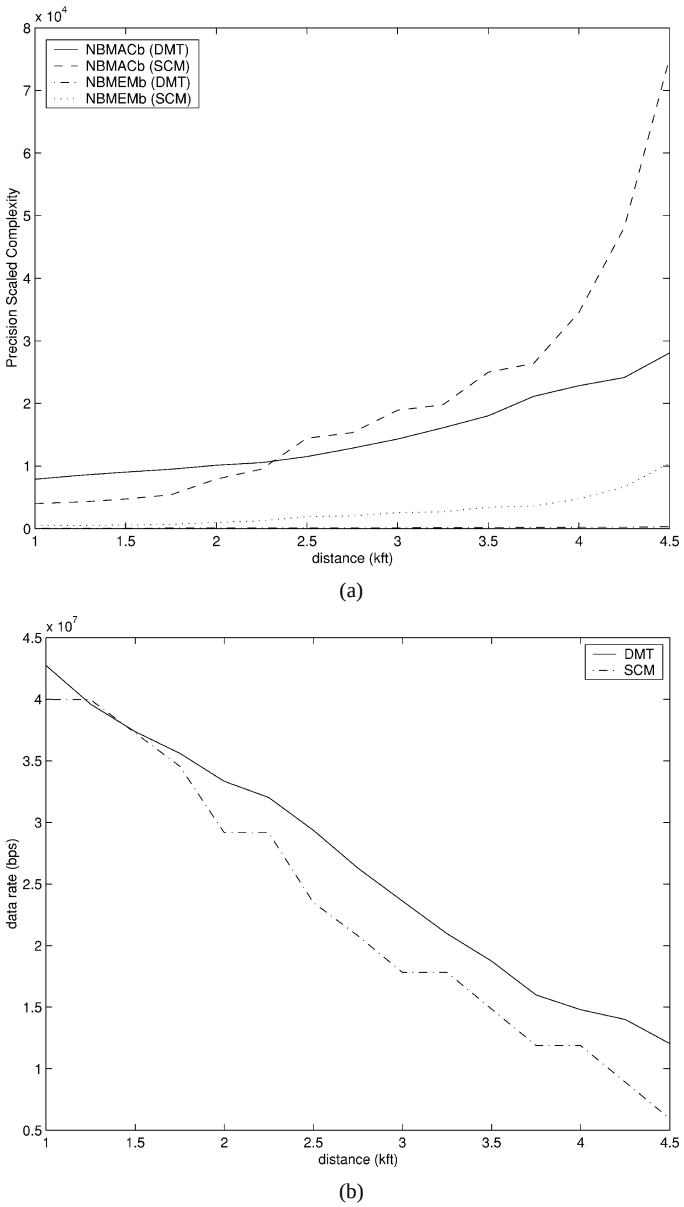

Fig. 12. Complexity metrics when amateur radio band interferer is present. (a) Precision scaled complexity metrics (NB_{MACb} and NB_{MEMb}). (b) Data rate (R_{DMT} and R_{SCM}).

−80 dBm/Hz [1]). As specified in the standard [1], downstream band1 overlaps with 1.8–2.0 and 3.5–4.0 MHz radio band and band3 overlaps with 7.0–7.3 MHz radio band.

To overcome this problem, the tone overlapping with the RFI band needs to be turned off in DMT transmitter. As the subcarrier in DMT has spectral leakage due to the imperfect band separation, we also turned off one additional tone on each side. In SCM transmitter, a second-order IIR notch filter is employed to reject RFI egress [35], which requires three additional MACs for each sample in the transmitter. For the RFI simulation, we included the RFI signal generated by double-sideband modulated Gaussian signal with a 4-kHz cutoff frequency. Fig. 12 shows the complexity and performance in the presence of RFI. Due to the large residual ISI caused by notching RFI, we can see that the performance of SCM degrades severely for a long distances. Note that the crossover distance at which DMT has lower computational complexity is now around 2 kft.

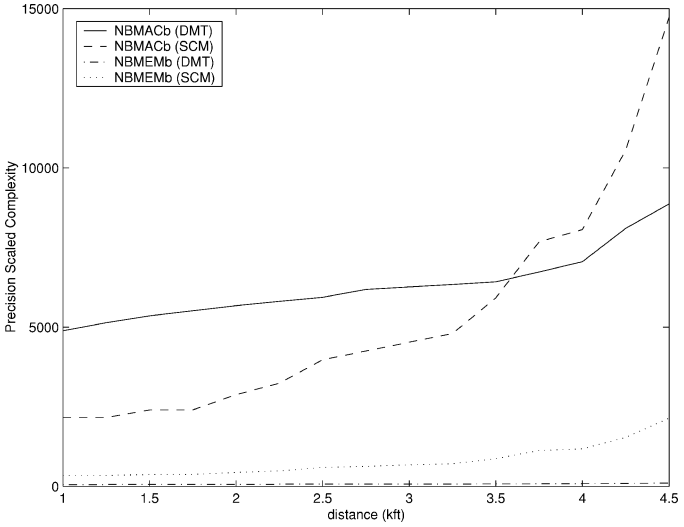

(a)

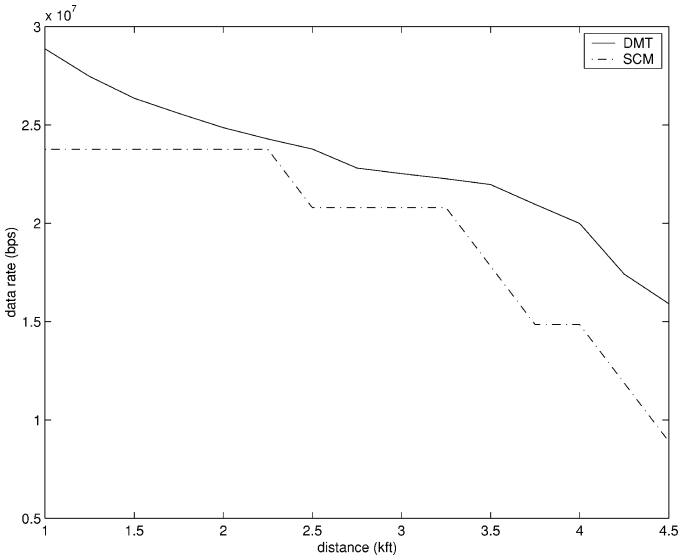

(b)

Fig. 13. Complexity metrics when using downstream band 1 only. (a) Precision scaled complexity metrics (NB_{MACb} and NB_{MEMb}). (b) Data rate (R_{DMT} and R_{SCM}).

Finally, we considered the case where only downstream 1 band (DS1) is employed. It is evident from the previous results that the performance degradation in a long distance channel is significant in both systems (especially for the high frequency band). Thus, only downstream band1 can be used in many practical situations for economic reasons. For the same channel configuration of Fig. 9, we employed 2048 tone in DMT and single transmitter for DS1 in SCM. As seen from Fig. 13, for both systems, we can observe the considerable improvement in efficiency compared with that of full band use shown in Fig. 9. It is also shown that SCM has lower computational complexity until 3.5 kft.

V. Conclusion

In this paper, we provided the system complexity analysis of two modulation scheme (DMT and SCM) for very high-speed digital subscriber line. By analyzing the transceiver complexity for the downstream direction of VDSL, we computed the arithmetic complexity expressed as multiply-and-accumulate (MAC) operation and memory requirements. In addition, we presented the rate normalized complexity (N_{MACb}) and precision scaled complexity (NB_{MACb}) in order to obtain more comprehensive metrics. While SCM has a smaller computational complexity in a loop with short distance, it is observed that DMT has smaller computational complexity in a long distance and complex channel as mixed gauge with bridge tap or RFI. The information presented in this paper can be used as a reference for other analysis such as complexity analysis in upstream direction, transceiver power estimation or can serve as a baseline in complexity analysis for other transmission channels.

Acknowledgment

The authors would like to thank the anonymous reviewers and the associate editor for their helpful suggestions that considerably improved the quality of this paper.

References

[1] "Very-high-speed digital subscriber line (VDSL) metallic interface, Part 1: Functional requirements and common specification," Amer. Nat. Stand. Inst., ANSI, T1E1.4/2001–009R2, 2001.

[2] "For telecommunications-network and customer installation interfaces-symmetrical digital subscriber line (ADSL) metallic interface," Amer. Nat. Stand. Inst., ANSI, T1E1.4/95–413, 1995.

[3] "VDSL metallic interface, Part 3: Technical specification of a multi-carrier modulation transceiver," Amer. Nat. Stand. Inst., ANSI T1E1.4/2001–013R1, 2001.

[4] "VDSL metallic interface. Part 2: Technical specification for an SCM transceiver," Amer. Nat. Stand. Inst., ANSI T1E1.4/2001–011R1, 2000.

[5] J. M. Cioffi, V. Oksman, J. Werner, T. Pollet, P. M. P. Spruyt, J. S. Chow, and K. S. Jacobsen, "Very-high-speed digital subscriber lines," *IEEE Commun. Mag.*, pp. 72–79, Apr. 1999.

[6] V. Oksman and J. J. Werner, "Single carrier modulation technology for very high-speed digital subscriber line," *IEEE Commun. Mag.*, pp. 82–89, May 2000.

[7] J. M. Cioffi, G. P. Dudevoir, M. V. Eyuboglu, and G. D. Forney, "MMSE decision-feedback equalizers and coding – Part I: Equalization results," *IEEE Trans. Commun.*, vol. 43, pp. 2582–2594, Oct. 1995.

[8] J. T. Aslanis and J. M. Cioffi, "Achievable information rates on digital subscriber loops: Limiting information rates with crosstalk noise," *IEEE Trans. Commun.*, vol. 40, pp. 361–372, Feb. 1992.

[9] D. Schmucking and A. Worner, "Transmission capacity and design of a VHDSL-system," in *Proc. IEEE Commun. Conf.*, vol. 3, 1996, pp. 1426–1431.

[10] D. M. Krinsky, D. E. Veeneman, and R. Olshansky, "Bandwidth selection for the very high-rate digital subscriber line system," in *Proc. IEEE Commun. Conf.*, vol. 3, 1996, pp. 1432–1436.

[11] S. Daigle and D. Falconer, "Evaluation of transmission alternatives for the return cable band," in *Proc. IEEE Commun. Conf.*, vol. 2, 1998, pp. 916–920.

[12] J. S. Chow, J. C. Tu, and J. Cioffi, "A discrete multitone transceiver system for HDSL application," *IEEE J. Selec. Areas Commun.*, vol. 9, pp. 895–908, Aug. 1991.

[13] J. M. Cioffi, "Line code complexity," Amer. Nat. Stand. Inst., ANSI T1E1.4/95–022, 1995.

[14] B. R. Saltzberg, "Comparison of single-carrier and multitone digital modulation for ADSL applications," *IEEE Commun. Mag.*, pp. 114–121, Nov. 1998.

[15] J. M. Cioffi, G. Ginis, and W. Yu, "Construction of modulated signals from filter bank elements and equivalence of line codes," Amer. Nat. Stand. Inst., ANSI T1E1.4/99–395, 1999.

[16] B. R. Wiese and J. S. Chow, "Programmable implementations of xDSL transceiver systems," *IEEE Commun. Mag.*, pp. 114–119, May 2000.

[17] E. O. Brigham, *The Fast Fourier Transform and Its Applications*. Englewood Cliffs, NJ: Prentice-Hall, 1988, pp. 191–193.

[18] T. Starr, J. Cioffi, and P. Silverman, *Understanding Digital Subscriber Line Technology*. Englewood Cliffs, NJ: Prentice-Hall, 1999.
[19] N. R. Shanbhag and M. Goel, "Low-power adaptive filter architectures and their application to 51.84 Mb/s ATM-LAN," *IEEE Trans. Signal Processing*, vol. 45, pp. 1276–1290, May 1997.
[20] D. Mesdagh and P. Spruyt, "A method to reduce the probability of clipping in DMT-based transceivers," *IEEE Trans. Commun.*, vol. 44, pp. 1234–1238, Oct. 1996.
[21] J. T. Tellado and J. M. Cioffi, "PAR reduction in multicarrier transmission systems," Amer. Nat. Stand. Inst., ANSI T1E1.4/97–367, 1998.
[22] A. V. Oppenheim and R. W. Schafer, *Discrete-Time Signal Processing*. Englewood Cliffs, NJ: Prentice-Hall, 1989, pp. 637–641.
[23] J. M. Labaey and M. Pedram, *Low Power Design Methodologies*. Boston, MA: Kluwer, 1996, pp. 160–200.
[24] R. D. Gitlin and S. B. Weinstein, "Fractionally-spaced equalization: An improved digital transversal equalizer," *Bell Syst. Tech. J.*, vol. 60, no. 2, pp. 275–296, Feb. 1981.
[25] L. M. Garth, J. Yang, and J. J. Werner, "Blind equalization algorithms with automatic constellation phase recovery for dual-mode CAP-QAM reception," in *Proc. IEEE Commun. Conf.*, vol. 3, 1999, pp. 1531–1536.
[26] G. H. Im and J. J. Werner, "Bandwidth-efficient digital transmission over unshielded twisted-pair wiring," *IEEE J. Select. Areas Commun.*, vol. 13, pp. 1643–1655, Dec. 1995.
[27] B. Daneshrad and H. Samueli, "A 1.6 Mb/s digital-QAM system for DSL transmission," *IEEE J. Select. Areas Commun.*, vol. 13, pp. 1600–1610, Dec. 1995.
[28] L. Erup, F. M. Gadner, and R. A. Harris, "Interpolation in digital modems – Part II : Implementation and performance," *IEEE Trans. Commun.*, vol. 41, pp. 998–1008, June 1993.
[29] V. Oksman, "Reducing ADC resolution by using analog band-pass filters in FDD based VDSL," Amer. Nat. Stand. Inst., ANSI T1E1.4/99–334, 1999.
[30] M. Goel and N. R. Shanbhag, "Finite-precision analysis of the pipelined strength-reduced adaptive filter," *IEEE Trans. Signal Processing*, vol. 46, pp. 1763–1769, June 1998.
[31] P. S. Chow, J. M. Cioffi, and J. A. C. Bingham, "A practical discrete multitone transceiver loading algorithm for data transmission over spectrally shaped channels," *IEEE Trans. Commun.*, vol. 43, pp. 773–775, Feb. 1995.
[32] J.-J. Werner, "The HDSL environment," *IEEE J. Select. Areas Commun.*, vol. 9, pp. 785–800, Aug. 1991.
[33] A. Wang, J.-J. Werner, and S. Kallel, "Effect of bridged taps on channel capacity at VDSL frequencies," in *Proc. IEEE Commun. Conf.*, 1999, pp. 236–245.
[34] P. A. Voois, I. Lee, and J. M. Cioffi, "The effect of decision delay in finite-length decision feedback equalizer," *IEEE Trans. Inform. Theory*, vol. 42, pp. 618–621, Mar. 1996.
[35] M. V. Dragosevic and S. S. Stankovic, "An adaptive notch filter with improved tracking properties," *IEEE Trans. Signal Processing*, vol. 43, pp. 2068–2078, Sept. 1995.

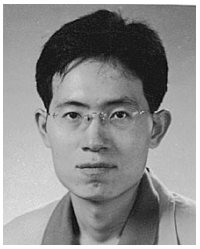

Byonghyo Shim received the B.S. and the M.S. degrees in control and instrumentation engineering from Seoul National University, Seoul, Korea, in 1995, 1997, respectively. He is currently pursuing the Ph.D. degree in electrical and computer engineering at University of Illinois at Urbana-Champaign.

From 1997 to 2000, he was a full-time instructor at the electronics engineering in Korean Air Force Academy, Cheonju. His research interests include signal processing for communication, VLSI signal processing, and low-power communication transceiver design.

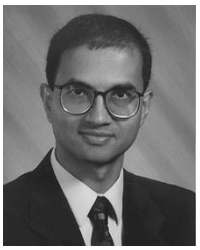

Naresh R. Shanbhag (M'93) received the B. Tech. degree from the Indian Institute of Technology, New Delhi, in 1988, the M.S. degree from the Wright State University, Dayton, OH, in 1990, and the Ph.D. degree from the University of Minnesota, Minneapolis, in 1993, all in electrical engineering.

From July 1993 to August 1995, he was with AT&T Bell Laboratories, Murray Hill, NJ, where he was responsible for the development of VLSI algorithms, architectures, and implementation of broadband data communications transceivers. In particular, he was the lead chip architect for AT&T's 51.84 Mb/s transceiver chips over twisted-pair wiring for asynchronous transfer mode (ATM)-LAN and broadband access chip sets. Since August 1995, he has been with the Department of Electrical and Computer Engineering and the Coordinated Science Laboratory, University of Illinois at Urbana-Champaign, where he is presently an Associate Professor and the Director of the Illinois Center for Integrated Microsystems. At the University of Illinois, he founded the VLSI Information Processing Systems (ViPS) Group, whose charter is to explore issues related to low-power, high-performance, and reliable integrated circuit implementations of broadband communications and digital signal processing systems. He has published more than 90 journal articles/book chapters/conference publications in this area and holds three U.S. patents. He is also a co-author of the research monograph entitles "Pipelined Adaptive Digital Filters" (Norwell, MA: Kluwer, 1994).

Dr. Shanbhag received the the 2001 IEEE Transactions on VLSI Systems Best Paper Award, the 1999 IEEE Leon K. Kirchmayer Best Paper Award, the 1999 Xerox Faculty Award, the National Science Foundation CAREER Award in 1996, and the 1994 Darlington Best Paper Award from the IEEE Circuits and Systems Society. From July 1997 to 2001, he was a Distinguished Lecturer for the IEEE Circuits and Systems Society. From 1997 to 1999, he served as an Associate Editor for the IEEE TRANSACTION ON CIRCUITS AND SYSTEMS: PART II. He is presently an Associate Editor for the IEEE TRANSACTIONS ON VLSI SYSTEMS. He has served on the technical program committee of various international conferences. He was the Technical Program Chair of the 2002 IEEE Workshop on Signal Processing Systems.